

Iridium-Catalysed C(sp^3)–H Activation and Hydrogen Isotope Exchange via Nitrogen-Based Carbonyl Directing Groups

Nathan M. L. Knight,^a James D. F. Thompson,^a John A. Parkinson,^a David M. Lindsay,^a Tell Tuttle,^a and William J. Kerr^{a,*}

^a Department of Pure and Applied Chemistry, University of Strathclyde, Glasgow G1 1XL, Scotland, U.K.
Fax: (+44)-141-548-4822
Phone: (+44)-141-548-2959
E-mail: w.kerr@strath.ac.uk

Manuscript received: February 9, 2024; Revised manuscript received: April 12, 2024;
Version of record online: ■■, ■■■

Supporting information for this article is available on the WWW under <https://doi.org/10.1002/adsc.202400156>

© 2024 The Authors. Advanced Synthesis & Catalysis published by Wiley-VCH GmbH. This is an open access article under the terms of the Creative Commons Attribution License, which permits use, distribution and reproduction in any medium, provided the original work is properly cited.

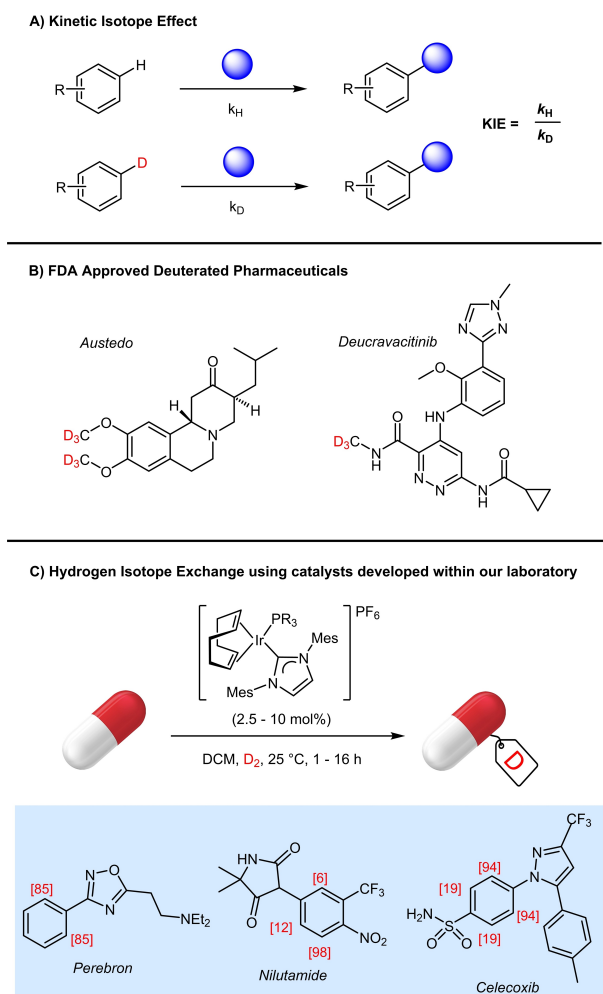
Abstract: Growing interest in improved structural diversity within the pharmaceutical industry has led to a focus on more sp^3 -rich drug frameworks. Meanwhile, spiralling pharmaceutical research and development costs continue to require expedited adsorption, distribution, metabolism, excretion, and toxicity studies, which are heavily reliant on the use of molecules incorporating deuterium and tritium. Herein, we report an iridium catalyzed C(sp^3)–H activation and hydrogen isotope exchange (HIE) methodology capable of utilizing pharmaceutically ubiquitous nitrogen-based carbonyl directing groups. High levels of deuterium incorporation (> 80% in 37 of the examples) are demonstrated across a range of substrates (5-, 6-, and 7-membered lactams, cyclic carbamates and ureas, acyclic amides), with tolerance of a range of common functional groups (aryl, alkoxy, halogen, ester, alcohol, sulfonamide) and predictable regioselectivity. The applicability of this methodology was demonstrated with up to 98% deuterium incorporation observed in a range of challenging bioactive molecules such as Nefiracetam, Praziquantel, and Unifiram. Density functional theory has provided mechanistic insight into the C–H activation and HIE at both the expected site of incorporation and an unexpected aryl labelling via a 7-membered metallocyclic intermediate.

Keywords: C–H activation; hydrogen isotope exchange; iridium; lactams; amides; pharmaceuticals

Introduction

Deuterated molecules have several key applications within the life sciences, most notably in absorption, distribution, metabolism, excretion, and toxicity (ADMET) studies,^[1] but also in mechanistic investigations *via* exploitation of the kinetic isotope effect (Scheme 1A).^[2,3] More recently, incorporation of deuterium has been used as a strategy to alter the metabolic profile of pharmaceuticals, such as in Austedo and Deucravacitinib, the first two FDA-approved deuterated pharmaceutical compounds (Scheme 1B).^[4,5] The widespread use of the hydrogen isotopes, deuterium (^2H or D) and tritium (^3H or T), is due in no small part to advances in the synthetic

accessibility of these isotopologues. In particular, installation *via* hydrogen isotope exchange (HIE)^[6,7] allows the late-stage incorporation of deuterium or tritium, and avoids time-consuming re-synthesis using expensive labelled substrates or reagents. Within our laboratories, a series of electron-rich, sterically encumbered iridium(I) NHC/phosphine catalysts have enabled the late-stage labelling of aromatic systems using a variety of directing groups (Scheme 1C),^[8,9] and including challenging aryl sulfonamides^[10] and *N*-heterocycles.^[11] Importantly, such catalysts facilitate HIE under mild conditions, with excellent functional group tolerance, and using deuterium gas as the isotope source, allowing the ready translation of these methods towards tritiation of drug-like compounds.^[8]



Scheme 1. A) Illustration of the kinetic isotope effect (KIE). B) The FDA approved pharmaceuticals, Austedo and Deucravacitinib. C) Examples of HIE of pharmaceuticals using $[\text{Ir}(\text{COD})(\text{IMes})(\text{PR}_3)]\text{PF}_6$ catalysts with deuterium gas. Deuterium incorporation denoted by [XX] at the position of incorporation.

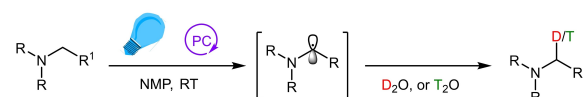
Within drug discovery, the pharmaceutical industry has traditionally focused on a subset of reliable transformations, including the Suzuki-Miyaura reaction and $\text{S}_{\text{N}}\text{Ar}$ processes.^[12] While these modular transformations facilitate rapid access to “drug-like” fragments, the repetitive use of these staple reactions has resulted in an overabundance of linear/planar, sp^2 -rich bioactive molecules being explored.^[13,14] Indeed, these sp^2 -rich frameworks have increasingly been linked with poor bioavailability and target promiscuity, resulting in a growing interest in three-dimensional, structurally diverse, natural product-like molecular frameworks,^[15–18] due to the improved biological effectiveness and lower toxicity as the fraction of sp^3 (F_{sp^3}) and chiral atom count increases. In addition, conducting ADMET studies earlier in the development lifecycle has been proposed as a key strategy to alleviate the escalating costs of pharmaceutical R&D

by reducing late-stage compound attrition.^[19,20] Isotopically labelled compounds play a pivotal role within ADMET studies, providing a molecular “tag” without significantly altering the physicochemical properties of the compounds,^[1] with the hydrogen isotopes being particularly appealing due to their high sensitivity of detection by mass spectrometry or scintillation, for deuterium and tritium, respectively.^[21] Despite the appreciable advances that have been accomplished within the field of HIE within the past > 20 years,^[6,7,22–25] HIE at sp^3 centres remains markedly underexplored despite the rapidly increasing interest in sp^3 -rich pharmaceutical frameworks.^[26]

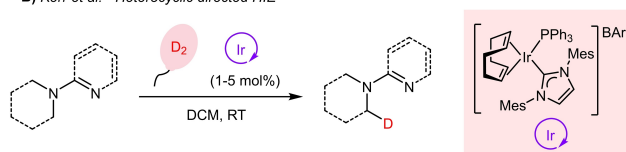
A small number of basic^[27] or heterogeneous catalysis approaches, either via supported catalysts^[28–29] or nanoparticles,^[30] have been reported for the labelling of specific $\text{C}(sp^3)\text{--H}$ bonds. However, in some cases, sub-optimal regioselectivity, limited functional group tolerance, the use of deuterated solvents, or elevated pressures, restricts the effectiveness of these methodologies, including any transference to tritiation processes. In contrast, reported homogeneous metal-catalysed HIE approaches can deliver highly selective methodologies, either based on the steric or electronic attributes of the target molecules,^[31] or *via ortho*-directed HIE,^[7] including a stereoretentive α -labelling of chiral amines using a ruthenium complex with D_2O as the isotope source.^[32] One notable report was published by MacMillan *et al.* in 2017, with the elegant use of photoredox catalysis to deuterate or tritiate amines at the α -position, using either D_2O or T_2O , respectively (Scheme 2A),^[33] and with excellent

Previous Work

A) Macmillan *et al.* - Amine directed HIE

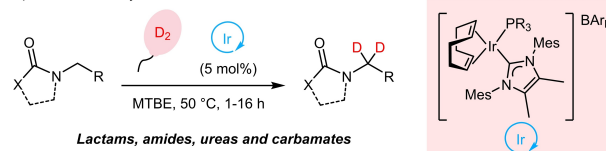


B) Kerr *et al.* - Heterocyclic directed HIE



This Work

C) General carbonyl directed HIE



Scheme 2. A–B) Notable examples of previously reported homogeneous sp^3 HIE. C) *This work*: a broadly applicable nitrogen-based carbonyl-directed sp^3 HIE.

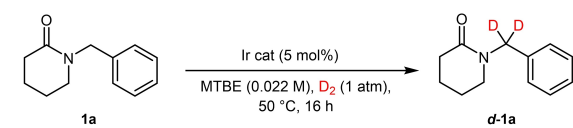
functional group tolerance exhibited across a diverse range of pharmaceutical frameworks under mild reaction conditions. Having stated this, within the pharmaceutical industry, T₂ is the preferred isotope source in the preparation of tritiated compounds due to its improved isotopic purity compared to alternative tritium sources.^[34] In this regard, Yang and Lehnher have reported a dual homogeneous/photoredox catalysis approach for labelling adjacent to amines that employs D₂ or T₂ as the isotope source.^[35]

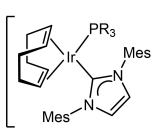
C(sp³)-H HIE has also been addressed within our laboratory, with the *N*-heteroaromatic-directed labelling of saturated *N*-heterocycles at room temperature, using just 1–5 mol% of our [Ir(COD)(IMes)(PPh₃)]BAR_F catalyst (Scheme 2B).^[36] While a range of different heteroaromatic directing groups and varied functional groups were well tolerated, these mild reaction conditions were not amenable to weaker, carbonyl-based directing groups. Related to this, Derdau and co-workers reported that the use of elevated temperatures and a higher loading (10 mol%) of the same catalyst facilitated the labelling of specific amide substrates, containing either (di)sulfides or protected glycine residues.^[37] Based on this, a mild and general C(sp³)-H HIE methodology targeting pharmaceutically ubiquitous nitrogen-based carbonyl directing groups is yet to be described. Herein, we report a broadly applicable, carbonyl-directed C(sp³)-H HIE protocol, where a novel iridium(I) NHC-phosphine catalyst furnishes high levels of deuterium incorporation under mild reaction conditions (Scheme 2C).

Results and Discussion

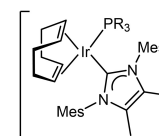
Given its ubiquity in bioactive molecules, we initially chose to target sp³ labelling directed by the lactam motif, focusing on the α-methylene position of the lactam sidechain. Accordingly, reaction exploration was initially conducted on *N*-benzyl valerolactam **1a**, due to the potentially beneficial benzylic activation and the constrained lactam directing group representing a privileged pharmaceutical scaffold (Table 1). Preliminary investigations were immediately promising: in MTBE at 50 °C under a D₂ atmosphere (balloon), use of the commercially available catalyst **2a** (5.0 mol%) furnished 58% deuterium incorporation (entry 1). Exchange of the phosphine ligand to the smaller, more electron-rich PMe₂Ph in catalyst **2b** resulted in a slight improvement in the deuteration to 64% (entry 2). A greater increase in deuterium incorporation was realized upon modification of the NHC ligand to the 4,5-dimethylated species, IMes^{Mes}, in novel catalysts **3a–3c** (entries 3–5), with [Ir(COD)(IMes^{Mes})(PBn₃)]BAR_F **3c** (entry 5) providing an excellent 92% deuterium incorporation. Notably, flexible, electron-rich trialkyl phosphine ligands delivered

Table 1. Catalyst optimization for the HIE of *N*-benzyl valerolactam **1a** in MTBE at 50 °C under a D₂ atmosphere (balloon). Results are an average of 2 reactions.

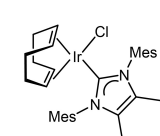




2a, PR₃ = PPh₃
2b, PR₃ = PMe₂Ph



3a, PR₃ = PPh₃
3b, PR₃ = PBu₃
3c, PR₃ = PBn₃



4a

| Entry | Catalyst | Deuterium Incorporation/% |
|------------------|-----------|---------------------------|
| 1 | 2a | 58 |
| 2 | 2b | 64 |
| 3 | 3a | 80 |
| 4 | 3b | 91 |
| 5 | 3c | 92 |
| 6 ^[a] | 3c | 15 |
| 7 ^[b] | 3c | 16 |
| 8 | 4a | 0 |

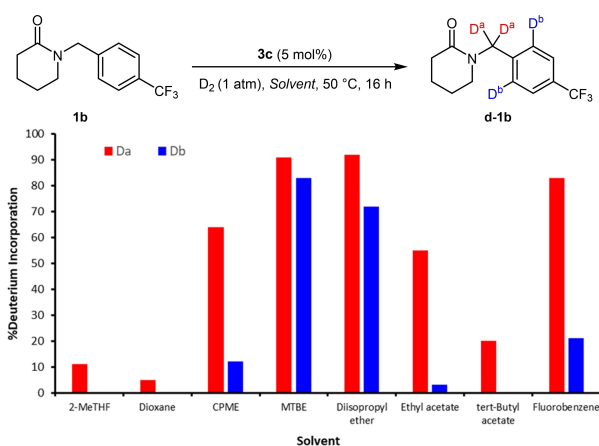
Deviation from standard conditions:

^[a] Concentration increased to 0.11 M,

^[b] Catalyst loading decreased to 2.5 mol%.

the greatest activity, with the use of **3b** (containing PⁿBu₃) resulting in only a slight reduction in deuterium incorporation, at 91%. Increasing the concentration of the HIE reaction to 0.11 M, or reducing the catalyst loading to 2.5 mol%, resulted in a significant reduction in catalytic activity (entries 6–7, respectively). Meanwhile, other iridium(I) pre-catalyst motifs, such as the iridium chlorocarbene **4a**, which has demonstrated significant HIE activity in previous work,^[10,38] proved to be completely inactive for this C(sp³)-H HIE procedure; we presume that this depleted chloro complex activity is based on the anticipated relatively higher energy of the alkyl iridacycle that would result from use of the more electron-rich neutral chlorocarbene species.

We next investigated the effect of substitution on the phenyl ring. On moving from the unsubstituted *N*-benzyl valerolactam **1a** to the *p*-CF₃-containing lactam **1b**, excellent levels of sp³ labelling were maintained (Scheme 3, solvent = MTBE). However, unexpectedly, aryl HIE was also observed at the position *ortho* to the lactam sidechain (D^o). This labelling is believed to proceed *via* a largely unprecedented 7-membered metallocyclic intermediate (7-mmⁱ),^[39] and opens up the additional possibility for 4 deuterium atoms to be installed using a single amide directing group, with potential application in the synthesis of stable isotopically-labelled standards (SILS), where M + 4 isotopo-



Scheme 3. Solvent optimization for the HIE of 4-(trifluoromethyl)benzylpiperidin-2-one **1b** at 50 °C using **3c** (5 mol%) under a D₂ atmosphere (balloon). Results are displayed as an average of at least 2 reactions.

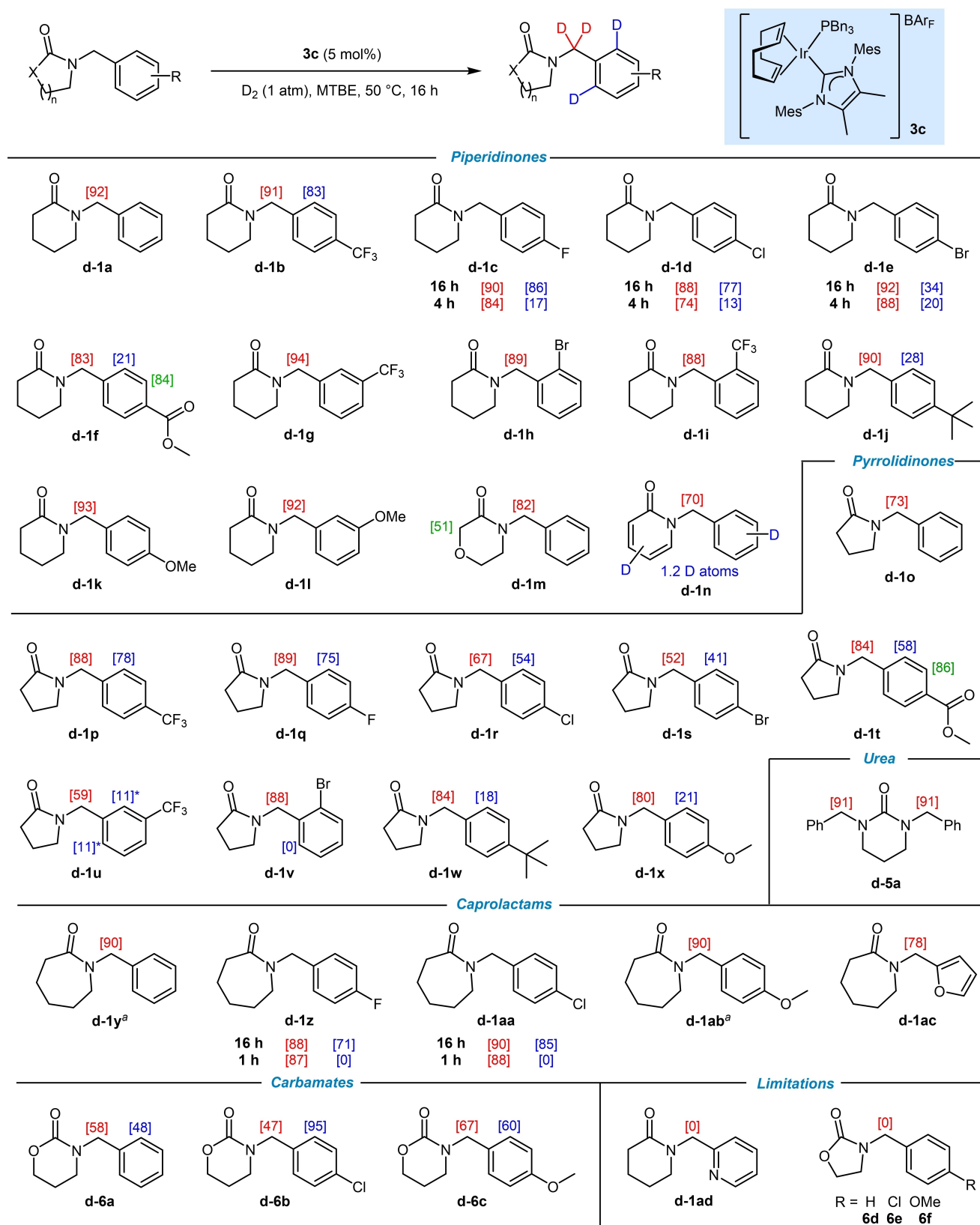
logues are often employed.^[1] An investigation into the solvent applicability of this methodology (Scheme 3) highlighted the unique efficiency of the ether solvents, with both MTBE and *i*-Pr₂O resulting in >90% *sp*³ benzylic incorporation and >70% aryl incorporation. In contrast, the use of fluorobenzene as solvent resulted in greater selectivity towards *Csp*³ deuterium incorporation, furnishing 83%D at this position (D_a) but only 20% deuterium incorporation at the aryl positions (D_b). Based on overall *sp*³ labelling efficiency, MTBE was selected as the optimal solvent for further investigations.

With optimized conditions in hand, the substrate scope for this transformation was explored through a wide range of benzylic lactams, with our developed HIE procedure furnishing good levels of benzylic deuterium incorporation across a variety of substituents and directing group ring sizes (Scheme 4). Starting with derivatives of *N*-benzyl valerolactam, electron-withdrawing (**1b–1i**) and electron-donating (**1j–1l**) substituents in the *para*-, *meta*-, or *ortho*-position were well tolerated, with ≥83% deuterium incorporation observed at the *sp*³ benzyl position in each instance. Interestingly, aryl labelling was only observed to a significant extent with substrates bearing electron-withdrawing substituents in the *para*-position (**1b–1f**) to the directing group. However, greater selectivity for the *sp*³ benzylic position could be realised by decreasing the reaction time to 4 h (**1c–1e**). Further derivatization of the lactam directing group was well tolerated, as demonstrated with the 3-morpholinone (**1m**) and pyridone (**1n**) derivatives. Changing from the 6-membered valerolactam directing group to a 5-membered pyrrolidone (**1o–1x**) resulted in very good levels of *sp*³ deuteration in the majority of examples. Certain substrates bearing electron-withdrawing groups (*p*-Cl

1r, *p*-Br **1s**, and *m*-CF₃ **1u**) did, nonetheless, deliver lowered levels of deuterium incorporations of 52–67%. In contrast, the 7-membered caprolactam-derived substrates (**1y–1ac**) provide generally excellent levels of labelling. Indeed, *sp*³ HIE was so facile with the caprolactam directing groups that complete benzylic selectivity could be achieved for **1z** and **1aa** by reducing the reaction time to 1 h in each case. The methodology was further applied to urea **5a** to yield an excellent 91% deuterium incorporation across both benzylic sites. Carbamates **6a–c** resulted in moderate levels of benzylic labelling, with these substrates also undergoing significant aryl deuteration, even with the *p*-methoxy arene substituent in **6c**. As also shown in Scheme 4, some carbonyl motifs were, however, not compatible with this methodology, including **1ad**, bearing a strongly coordinating pyridine unit, and the 5-membered oxazolidinones **6d–6f**.

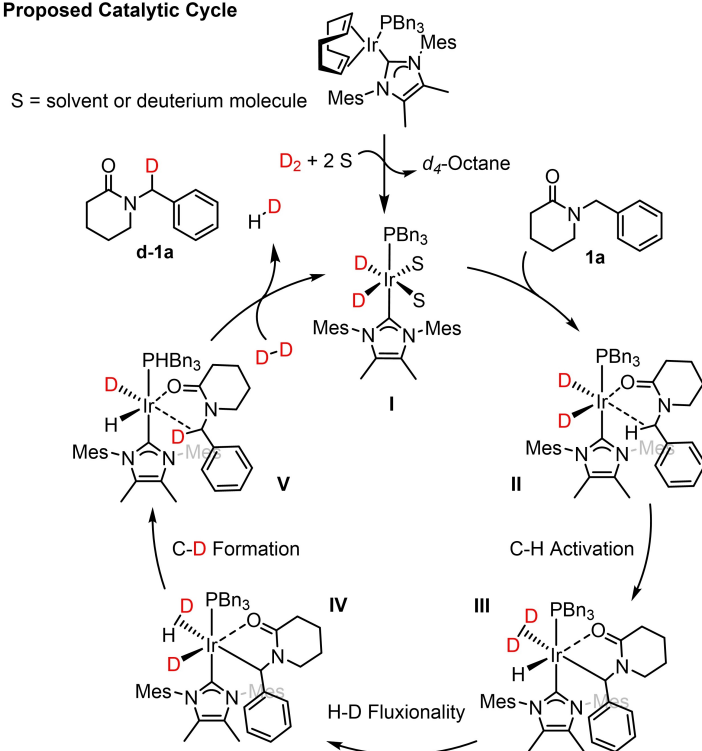
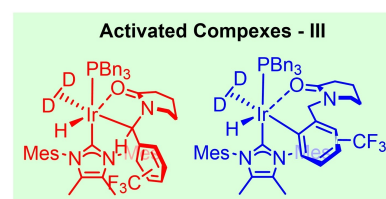
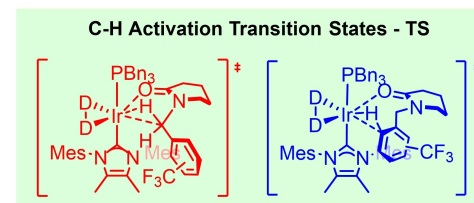
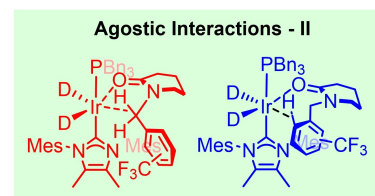
DFT studies have also been used to further probe the established C(*sp*³)-H activation and HIE process, and, in particular, to investigate the intriguing additional aryl deuterium incorporation observed in the presence of electron-withdrawing, *para*-substituted *N*-benzyl lactams. Specifically, key intermediates were calculated for the *ortho*-, *meta*-, and *para*-trifluoromethyl-substituted *N*-benzyl valerolactam substrates (**1i**, **1g**, and **1b**, respectively), in order to explore the factors determining why only *para*-substitution resulted in aryl labelling. The catalytic cycle is shown in Figure 1A and is adapted from the previously proposed mechanism, based on experimental and computational studies.^{8,35} Firstly, the pre-catalyst is activated by reduction of the cyclooctadiene ligand with D₂, to yield intermediate **I**. Substrate complexation occurs *via* coordination to the Lewis basic carbonyl directing group, and the key agostic interaction is then formed at the benzylic position, leading to intermediate **II**. C–H activation then furnishes the iridacycle intermediate **III**, which can undergo hydrogen fluxionality to yield species **IV**. Subsequent C–D bond formation and substrate decomplexation delivers the labelled product and returns the active catalyst **I**.

Our calculations focused on the key intermediates and transition states leading to the C–H activation for each of the C(*sp*³)-H and aryl-H labelling pathways, as illustrated in Figure 1B: the complexed substrates **II**, the C–H activation transition states **TS**, and the C–H activated complexes **III**, for each of the *p*-, *m*-, and *o*-CF₃ substrates **1b**, **1g**, and **1i**, respectively. For the *m*-CF₃ derivative **1g**, the calculations correspond to the least hindered of the two *ortho*-positions. Whilst 5-membered metallocyclic intermediates are well-precedented and, indeed, lead to benzylic deuterium incorporation in these substrates, the 7-membered metallocyclic analogue required for the observed aryl deuteration was perceived to be appreciably more



Scheme 4. Substrate scope for the HIE of *N*-benzyl lactams using $[\text{Ir}(\text{COD})(\text{IMes}^{\text{Me}})(\text{PBn}_3)]\text{BAR}_f$ (5 mol%) **3c** in MTBE at 50 °C for 16 h under an atmosphere of D_2 (balloon). [XX] denotes the level of deuterium incorporation at the indicated position. Each result is the average of at least two experiments. *Indicates an average incorporation across non-equivalent positions due to overlapping signals in the ^1H NMR spectrum. ^a1 h reaction time.

A) Proposed Catalytic Cycle

B) Key Intermediates and Transition State (II \rightarrow III)

C) Benzylic vs Aryl HIE

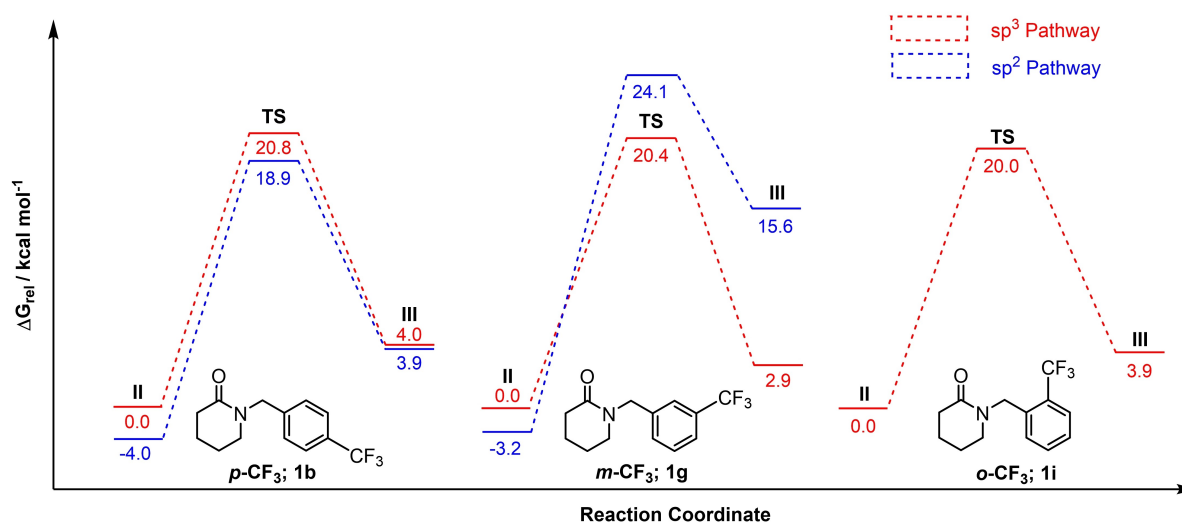


Figure 1. A) Proposed catalytic cycle. B) Key intermediates and transition states considered for the HIE of the benzylic and aryl positions for the CF_3 -containing substrates **1b**, **1g**, and **1i**. C) Partial potential energy surface for the C–H activation of the CF_3 -containing substrates **1b**, **1g**, and **1i** at both the benzylic and aryl positions, with the calculations conducted using M06 L/6–311G(d,p) for all non-Ir atoms and the Stuttgart-Dresden ECP for Ir. For each set of calculations for the three substrates, the zero point energy was set in each instance to the corresponding $\text{C}(sp^3)\text{-H}$ agostic complex.

challenging. Therefore, we were surprised to discover that the aryl C–H activation transition state energy barrier for the $p\text{-CF}_3$ substrate **1b** was $22.9 \text{ kcal mol}^{-1}$, only $2.1 \text{ kcal mol}^{-1}$ higher in energy than the corresponding $\text{C}(sp^3)\text{-H}$ benzylic transition state (Figure 1C), readily explaining the high levels of deute-

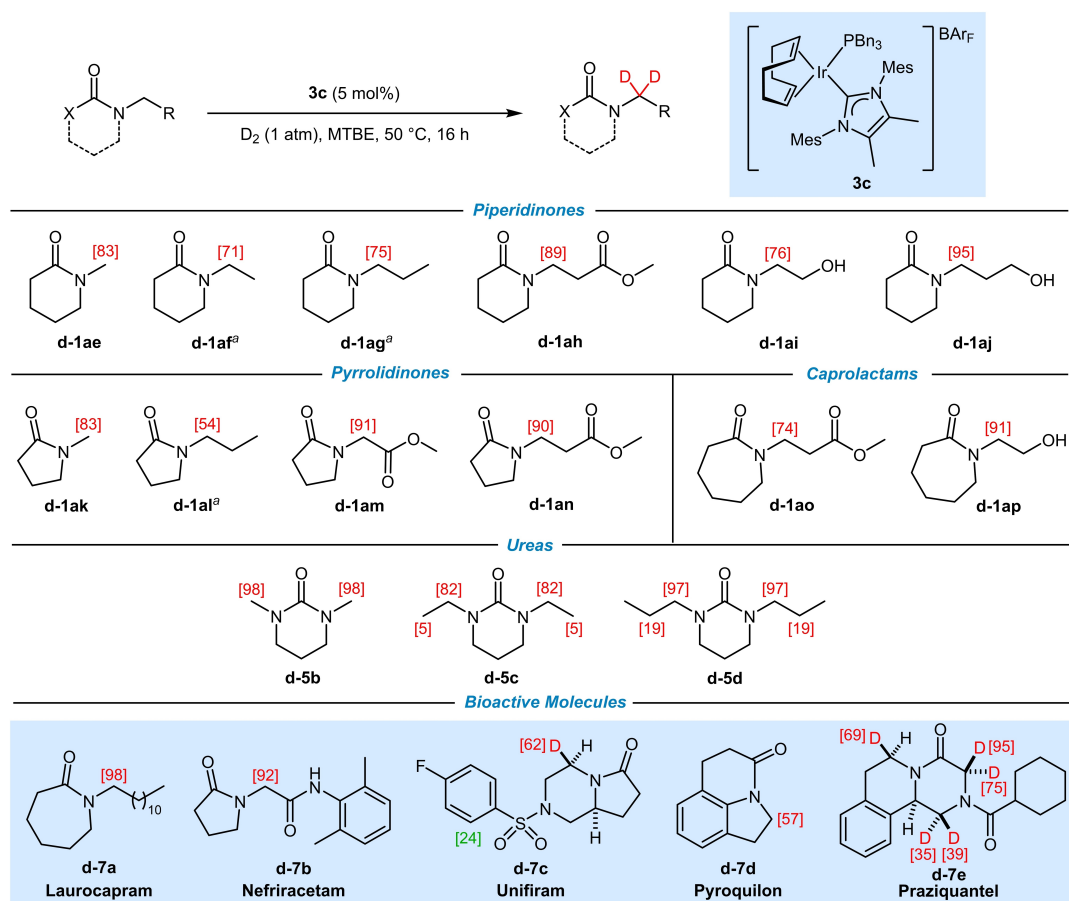
rium incorporation observed across both positions for this substrate. Furthermore, the energy for benzylic sp^3 C–H activation in each substrate (**1b**, **1g**, and **1i**) remains within a $\sim 1 \text{ kcal mol}^{-1}$ range, at $20.0\text{--}20.8 \text{ kcal mol}^{-1}$. This is consistent with the experimental results that show uniformly high levels of benzylic

deuterium incorporation across these three substrates. In contrast, for the *m*-CF₃-containing substrate **1g**, the transition state energy barrier for 7-*mmi* aryl C–H activation is significantly higher at 27.3 kcal mol⁻¹. This difference supports the complete regioselectivity observed in the HIE of the *meta*-substituted *N*-benzyl lactam. Importantly, the aryl agostic complex intermediates **II**_{Aryl} for *m*-CF₃ **1g** and *p*-CF₃ **1b** are comparable in energy to the corresponding benzylic agostic complexes (0.0 vs –3.2 and –4.0 kcal mol⁻¹, respectively). These similarities imply that the significant increase in the C–H activation transition state for *m*-CF₃ **1g** is related to the more disfavored iridacycle species **III**_{Aryl}.

Finally, the key C(*sp*²)–H agostic interaction in intermediate **II** for the *o*-CF₃ substrate **1i** could not be obtained due to the calculations converging to an interaction of the iridium centre with the π -system of the arene, centred on the *ortho*-aryl carbon (see ESI Section 2.3 for details). This change in behavior is likely due to the steric interaction between the *ortho*-substituent and the lactam ring, an interaction which is

impossible to avoid in the conformation required for the aryl C–H agostic complex. In comparison, the iridium– π system interaction requires a perpendicular arrangement of the arene and lactam ring systems, dramatically reducing the steric clash.

Following this study of *N*-benzyl lactam labelling reactive pathways, we next looked to broaden the scope of our HIE process further. Accordingly, we applied our developed method to a variety of non-benzylic lactam and urea substrates, as detailed in Scheme 5. Pleasingly, a good range of functionality was tolerated, including a range of alkyl chain lengths (**1ae–1ag** and **1ak–1al**), esters (**1ah**, **1am**, **1an**, and **1ao**), and alcohols (**1ai**, **1aj**, and **1ap**), across a variety of different ring sizes. Small alkyl side chains (**1af**, **1ag**, and **1al**) similarly proved resistant to this methodology, with a further short investigation and optimization (see ESI Section 1.3.5) discovering that more electron-rich catalysts could improve the level of deuterium incorporation observed. Accordingly, as indicated in Scheme 5, changing to the electron-rich catalyst [Ir(COD)(IMes^{Me})(PBu₃)]BAR_F **3b** resulted in



Scheme 5. HIE of further substrates *via* cyclic carbonyl directing groups. [XX] denotes the level of deuterium incorporation at the indicated position. Each result is the average of at least two experiments. ^a[Ir(COD)(IMes^{Me})(PBu₃)]BAR_F **3b** (5 mol%) used instead of **3c**.

a significant improvement in deuterium incorporation for these *N*-alkyl substrates. Urea directing groups also proved to be particularly amenable to this methodology, furnishing 82%–98% deuterium incorporation at the α -CH₂/CH₃ position in **5b–d**. As detailed in Scheme 5, the propyl-substituted **5d** also gave 19% deuterium incorporation in the β -position, likely proceeding through the energetically less favourable 6-membered metallocyclic intermediate. A selection of bioactive compounds was also subjected to the HIE methodology, including the percutaneous enhancer, Laurocapram **7a**; the nootropics, Nefiracetam **7b** and Unifiram **7c**; the fungicide, Pyroquilon **7d**; and the anti-parasitic agent, Praziquantel **7e**, with pleasing levels of deuterium incorporation observed even in strained polycyclic systems **7c**, **7d**, and **7e**. Interestingly, with both Unifiram **7c** and Praziquantel **7e**, the concave nature of the bicyclic system leads to exchange selectivity between diastereotopic C–H positions and, in particular, at one of the two methylene C–H bonds adjacent to the amide nitrogen.

Lastly, a small set of acyclic substrates were examined to evaluate the amide directing group in these cases (Scheme 6). Using the electron-rich catalyst [Ir(COD)(IMes^{Me})(P(*p*-MeOC₆H₄)₃)]BAR_F **3d**, high levels of deuterium incorporation ($\geq 80\%$) were obtained in each case. Notably, more sterically-congested methine C–H bonds could also be readily activated. Specifically, an excellent 95% deuterium incorporation was observed at the methine C–H of pivalamide **8c**, with 72% deuterium incorporation also occurring at the more remote and sterically hindered methine C–H of pivalamide **8d**, the latter *via* a less

favourable 6-membered metallocyclic intermediate. In both cases, labelling was also observed at the methyl groups of the pivalamide moiety.

Conclusion

In summary, we have established a method for C(*sp*³)-H activation and HIE *via* a variety of nitrogenous carbonyl-based directing groups to furnish isotopically-enriched products, using novel electron-rich and sterically encumbered iridium catalysts (**3c**, as well as **3b** and **3d**, at 5.0 mol%). The developed methodology tolerates several common functional groups (aryl, alkoxy, halogen, ester, alcohol, sulfonamide), and is applicable to a range of *N*-heterocycle ring sizes, with reactivity demonstrated across 57 examples, including 5 bioactive molecules. It is also anticipated that this methodology should prove translatable to late-stage pharmaceutical tritiation by pharmaceutically-aligned stakeholders, due to the compatibility of the developed method (temperature and gaseous isotope source) with preferred tritiation conditions.

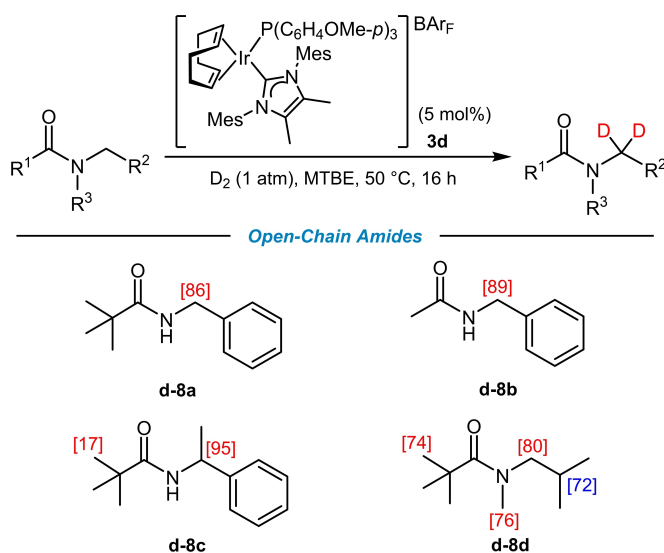
Experimental Section

Computational Methods

Density functional theory (DFT) was employed to calculate the electronic structures and energies for all species involved in H/D exchange reactions. A hybrid meta-GGA exchange correlation functional M06L was used in conjunction with the 6-311G(d,p) basis set for main group non-metal atoms, and the Stuttgart RSC effective core potential, along with the associated basis set, for Ir. Harmonic vibrational frequencies were calculated (with the incorporation of deuterium wherever needed) at the same level of theory to characterise respective minima (reactants, intermediates, and products with no imaginary frequency) and first order saddle points (TSs with one imaginary frequency). All calculations have been performed with the GAUSSIAN 16 quantum chemistry programme package. More detailed discussion of the computational methods, with full references, can be found in the Supporting Information.

General Procedure for the Synthesis of NHC/Phosphine Iridium(I) Complexes, [(COD)Ir-(PR₃)(NHC)] BAR_F

A flame-dried Schlenk tube under an argon atmosphere was charged with chlorocarbene complex [(COD)Ir(NHC)Cl] (1 eq.) and NaBAR_F (1 eq.) and the solids were stirred under vacuum for 10 min. The solids were subjected to an argon atmosphere before DCM (30 mL/mmol of [(COD)Ir(NHC)Cl] complex) was added slowly. The resultant solution was stirred for 30 min before the requisite phosphine (1 eq.) was added, and the reaction mixture was stirred for 16 h. The solvent was removed under reduced pressure and the residue was purified using flash column chromatography (silica gel, 50% DCM/petroleum ether, then DCM) to yield the desired catalysts.



Scheme 6. HIE of aliphatic substrates *via* amide directing groups. [XX] denotes the level of deuterium incorporation at the indicated position. Each result is the average of at least two experiments.

General Procedure for Hydrogen Isotope Exchange

12 oven-dried Radley carousel tubes were cooled under vacuum and backfilled with argon. Each tube was charged with the substrate (0.108 mmol) and iridium catalyst. The requisite solvent was added, and the reactions tubes were cooled to -78°C . The tubes were evacuated and backfilled with deuterium gas through 3 cycles. The tubes were then sealed and warmed to 50°C for the allocated reaction time. The reaction mixtures were cooled to room temperature and the solvent was removed under reduced pressure. The residue was dissolved in DCM (2 mL) and filtered through a silica plug (10 mL), which was then washed with DCM and then 5% methanol/DCM. The washes were combined, and the solvent was removed under reduced pressure to yield the deuterated product.

Deuterium incorporation was determined using ^1H NMR spectroscopy. The residual proton signal from the site of incorporation was compared to a position where incorporation was not expected or occurred.

Full compound characterization, experimental procedures, and DFT calculations can be found in the Supporting Information.

Acknowledgements

We thank the University of Strathclyde for PhD studentship funding, and GSK for additional PhD student support.

References


- [1] J. Atzrodt, V. Derdau, W. J. Kerr, M. Reid, *Angew. Chem. Int. Ed.* **2018**, *57*, 1758–1784.
- [2] J. E. Baldwin, *J. Labelled Compd. Radiopharm.* **2007**, *50*, 947–960.
- [3] E. M. Simmons, J. F. Hartwig, *Angew. Chem. Int. Ed.* **2012**, *51*, 3066–3072.
- [4] C. Schmidt, *Nat. Biotechnol.* **2017**, *35*, 493.
- [5] S. M. Hoy, *Drugs* **2022**, *82*, 1671–1679.
- [6] a) J. Atzrodt, V. Derdau, W. J. Kerr, M. Reid, *Angew. Chem. Int. Ed.* **2018**, *57*, 3022–3047; b) S. Kopf, F. Bourriquen, W. Li, H. Neumann, K. Junge, M. Beller, *Chem. Rev.* **2022**, *122*, 6634–6718.
- [7] W. J. Kerr, G. J. Knox, L. C. Paterson, *J. Labelled Compd. Radiopharm.* **2020**, *63*, 281–295.
- [8] J. A. Brown, A. R. Cochrane, S. Irvine, W. J. Kerr, B. Mondal, J. A. Parkinson, L. C. Paterson, M. Reid, T. Tuttle, S. Andersson, G. N. Nilsson, *Adv. Synth. Catal.* **2014**, *356*, 3551–3562.
- [9] A. R. Kennedy, W. J. Kerr, R. Moir, M. Reid, *Org. Biomol. Chem.* **2014**, *12*, 7927–7931.
- [10] W. J. Kerr, M. Reid, T. Tuttle, *ACS Catal.* **2015**, *5*, 402–410.
- [11] a) W. J. Kerr, D. M. Lindsay, P. K. Owens, M. Reid, T. Tuttle, S. Campos, *ACS Catal.* **2017**, *7*, 7182–7186; b) J. Atzrodt, V. Derdau, W. J. Kerr, M. Reid, P. Rojahn, R. Weck, *Tetrahedron* **2015**, *71*, 1924–1929.
- [12] D. G. Brown, J. Boström, *J. Med. Chem.* **2016**, *59*, 4443–4458.
- [13] F. Lovering, J. Bikker, C. Humblet, *J. Med. Chem.* **2009**, *52*, 6752–6756.
- [14] F. Lovering, *MedChemComm* **2013**, *4*, 515–519.
- [15] A. D. Morley, A. Pugliese, K. Birchall, J. Bower, P. Brennan, N. Brown, T. Chapman, M. Drysdale, I. H. Gilbert, S. Hoelder, A. Jordan, S. V. Ley, A. Merritt, D. Miller, M. E. Swarbrick, P. G. Wyatt, *Drug Discovery Today* **2013**, *18*, 1221–1227.
- [16] B. Over, S. Wetzel, C. Grütter, Y. Nakai, S. Renner, D. Rauh, H. Waldmann, *Nat. Chem.* **2013**, *5*, 21–28.
- [17] P. Arya, R. Joseph, Z. Gan, B. Rakic, *Chem. Biol.* **2005**, *12*, 163–180.
- [18] S. L. Schreiber, *Science* **2000**, *287*, 1964–1969.
- [19] D. Schuster, C. Laggner, T. Langer, *Curr. Pharm. Des.* **2005**, *11*, 3545–3559.
- [20] J. A. DiMasi, H. G. Grabowski, R. W. Hansen, *J. Health Econ.* **2016**, *47*, 20–33.
- [21] P. Hein, M. C. Michel, K. Leineweber, T. Wieland, N. Wettschreck, S. Offermanns, Receptor and Binding Studies. In *Practical Methods in Cardiovascular Research*, (Eds.: S. Dhein, F. W. Mohr, M. Delmar) Springer, Heidelberg, **2005**, pp. 723–783.
- [22] D. Hesk, *J. Labelled Compd. Radiopharm.* **2020**, *63*, 247–265.
- [23] T. Junk, W. J. Catallo, *Chem. Soc. Rev.* **1997**, *26*, 401–406.
- [24] W. J. S. Lockley, J. R. Heys, *J. Labelled Compd. Radiopharm.* **2010**, *53*, 635–644.
- [25] G. Prakash, N. Paul, G. A. Oliver, D. B. Werz, D. Maiti, *Chem. Soc. Rev.* **2022**, *51*, 3123–3163.
- [26] M. Valero, V. Derdau, *J. Labelled Compd. Radiopharm.* **2020**, *63*, 266–280.
- [27] a) Y. Hu, L. Liang, W.-T. Wei, X. Sun, X.-J. Zhang, M. Yan, *Tetrahedron* **2015**, *71*, 1425–1430; for a cesium base-mediated conversion of ArCH_3 to ArCD_3 , see: b) H.-Z. Du, J. Z. Fan, Z.-Z. Wang, N. A. Strotman, H. Yang, B.-T. Guan, *Angew. Chem. Int. Ed.* **2023**, *62*, e202214461.
- [28] a) H. Sajiki, F. Aoki, H. Esaki, T. Maegawa, K. Hirota, *Org. Lett.* **2004**, *6*, 1485–1487; for the general labelling of benzylic positions using Pd nanoparticles, see: b) V. Pfeifer, T. Zeltner, C. Fackler, A. Kraemer, J. Thoma, A. Zeller, R. Kiesling, *Angew. Chem. Int. Ed.* **2021**, *60*, 26671–26676.
- [29] A. Michelotti, F. Rodrigues, M. Roche, *Org. Process Res. Dev.* **2017**, *21*, 1741–1744.
- [30] a) G. Pieters, C. Taglang, E. Bonnefille, T. Gutmann, C. Puente, J.-C. Berthet, C. Dugave, B. Chaudret, B. Rousseau, *Angew. Chem. Int. Ed.* **2014**, *53*, 230–234; b) E. Levernier, K. Tatoueix, S. Garcia-Argote, V. Pfeifer, R. Kiesling, E. Gravel, S. Feuillastre, G. Pieters, *JACS Au* **2022**, *2*, 801–808; c) H. Kramp, R. Weck, M. Sandvoss, A. Sib, G. Mencia, P.-F. Fazzini, B. Chaudret, V. Derdau, *Angew. Chem. Int. Ed.* **2023**, *62*, e202308983; d) L. Neubert, D. Michalik, S. Bähn, S. Imm, H. Neumann, J. Atzrodt, V. Derdau, W. Holla, M. Beller, *J. Am. Chem. Soc.* **2012**, *134*, 12239–12244.

- [31] a) R. P. Yu, D. Hesk, N. Rivera, I. Pelczer, P. J. Chirik, *Nature* **2016**, *529*, 195–199; b) C. Zarate, H. Yang, M. J. Bezdek, D. Hesk, P. J. Chirik, *J. Am. Chem. Soc.* **2019**, *141*, 5034–5044.
- [32] L. V. A. Hale, N. K. Szymczak, *J. Am. Chem. Soc.* **2016**, *138*, 13489–13492.
- [33] Y. Y. Loh, K. Nagao, A. J. Hoover, D. Hesk, N. R. Rivera, S. L. Colletti, I. W. Davies, D. W. C. MacMillan, *Science* **2017**, *358*, 1182–1187.
- [34] R. Voges, J. R. Heys, T. Moenius, *Preparation of Compounds Labeled with Tritium and Carbon-14*, John Wiley & Sons, Chichester, **2009**.
- [35] H. Yang, Z. Huang, D. Lehnerr, Y.-H. Lam, S. Ren, N. A. Strotman, *J. Am. Chem. Soc.* **2022**, *144*, 5010–5022.
- [36] W. J. Kerr, R. J. Mudd, M. Reid, J. Atzrodt, V. Derdau, *ACS Catal.* **2018**, *8*, 10895–10900.
- [37] a) M. Valero, R. Weck, S. Güssregen, J. Atzrodt, V. Derdau, *Angew. Chem. Int. Ed.* **2018**, *57*, 8159–8163; see also: b) M. Valero, D. Becker, K. Jess, R. Weck, J. Atzrodt, T. Bannenberg, V. Derdau, M. Tamm, *Chem. Eur. J.* **2019**, *25*, 6517–6522.
- [38] A. R. Cochrane, S. Irvine, W. J. Kerr, M. Reid, S. Andersson, G. N. Nilsson, *J. Labelled Compd. Radiopharm.* **2013**, *56*, 451–454.
- [39] For a review of remote C–H activation, see: G. Meng, N. Y. S. Lam, E. L. Lucas, T. G. Saint-Denis, P. Verma, N. Chekshin, J.-Q. Yu, *Chem. Rev.* **2020**, *120*, 10571–10591.

RESEARCH ARTICLE

Iridium-Catalysed C(*sp*³)-H Activation and Hydrogen Isotope Exchange via Nitrogen-Based Carbonyl Directing Groups

Adv. Synth. Catal. **2024**, *366*, 1–11

 N. M. L. Knight, J. D. F. Thompson, J. A. Parkinson, D. M. Lindsay, T. Tuttle, W. J. Kerr*

